

FFC CAMBRIDGE PROCESS AND METALLIC 3D PRINTING FOR DEEP IN-SITU RESOURCE UTILISATION – A MATCH MADE ON THE MOON

A. Alex Ellery^{a*}, Paul Lowing^b, Priti Wanjara^c, Mark Kirby^d, Ian Mellor^b, Greg Doughty^b

^a Department of Mechanical and Aerospace Engineering, Carleton University, 1125 Colonel By Drive, Ottawa, Ontario, Canada, K1S 5B6, aellery@mae.carleton.ca

^b Metalysis Ltd, 2 Fairfield Park, Manvers Way, Wath upon Dearne, Rotherham, UK, S63 5DB, paul.lowing@metalysis.com; ian.mellor@metalysis.com; greg.doughty@metalysis.com

^c National Research Council, Aerospace Structures Materials & Manufacturing, University of Montreal, 5145 Decelles Avenue, Montreal, QC, Canada, H3T 2B2, Priti.Wanjara@cnrc-nrc.gc.ca

^d Renishaw Canada Ltd, 2196 Dunwin Drive, Mississauga, ON, Canada, L5L 1C7, mark.kirby@renishaw.com

* Corresponding Author

Abstract

Most in-situ resource utilisation (ISRU) techniques proposed to date are focussed on the extraction of consumables requiring minimal processing for the support of human missions to the Moon or Mars. Water in particular has been the beguiling jewel to which we have been drawn. We define this as shallow ISRU to illustrate that its extraction requires minimal processing. We are interested in deep ISRU – investing in the hard problem of extraction and processing of material that permits us to create physical infrastructure on the Moon. We submit that a new approach to space exploration beckons in which deep ISRU permits the robotic construction of an entire automated infrastructure on the Moon at low cost. By leveraging the enormous resources available of the Moon, the cost of human lunar missions can be reduced substantially. Our hypothesis is that following resource acquisition by bucket wheel, comminution and electrostatic/magnetic beneficiation, lunar regolith can be subjected to the FFC Cambridge process followed by 3D printing using either selective laser sintering or electron beam freeform fabrication. The FFC Cambridge process is an electrolytic technique that can extract near pure metals from their oxide and silicate forms. The two lunar minerals on which we have focussed are anorthite (common in the highland regions) and ilmenite (common in the maria regions). From these two minerals, an entire suite of metals can be extracted in alloy form, or if subjected to prior purification methods, in pure form – Al, Ca, Si from anorthite and Fe and Ti from ilmenite in alloy forms, or pure Al from alumina, pure Ti from rutile and pure Si from silica. The CaCl_2 electrolyte is recycled requiring only Cl import from Earth in salt form to replenish small losses. Furthermore, the output of the FFC Cambridge process is powder (or wire) suitable as input for powder metallurgy and metal 3D printing by electron beam freeform fabrication and selective laser sintering. Essentially, only two processes – FFC Cambridge and metal 3D printing – converts beneficiated raw material into final products. These two methods offer unprecedented capabilities in deep ISRU.

Keywords: In-situ resource utilization, FFC Cambridge process, 3D printing

1. Introduction

For long duration life support systems, it is considered essential to recycle everything to maximise consumption efficiency and minimise waste – this is the closed ecological life support system (CELSS). The term ecology implies a closed recycling system to re-use consumables. For example, solid state electrolysis may be used to recover oxygen from carbon dioxide and water (artificial photosynthesis): $2\text{CO}_2 \rightarrow 2\text{CO} + \text{O}_2$ and $2\text{H}_2\text{O} \rightarrow 2\text{H}_2 + \text{O}_2$. A number of suitable solid state electrolytes include calcia-stabilised zirconia or yttria-doped ceria at 850°C with an electrical energy consumption of 250 W. However, current environment control and life support systems (ECLSS) do not offer full closed loop recycling. Both ECLSS and CELSS must be supplemented by in-situ resource utilisation (ISRU) to supply raw materials for consumption and to

replace inevitable losses. For this reason, most ISRU techniques proposed to date have been devoted to the supply of consumables – water and oxygen. This is shallow ISRU.

Deep ISRU relates to more extensive use of space resources to support the in-situ construction, maintenance, repair and growth of infrastructure such as lunar habitats. Our interest is in building a self-replicating machine on the Moon entirely from lunar resources. This imposes a severe objective of a near-100% supply from in-situ resources. In fact, the scheme presented here requires the import of NaCl from Earth as a reagent (salt contingency). As humans begin to colonise the surface of the Moon and other planets, do we wish to bring our profligate habits with us? We have unfortunately begun by trailing our detritus into space up to GEO in the form of space debris. As we progress

beyond GEO to the Moon and other celestial bodies, we must commit to sustainable exploration.

2. Lunar Geology

Lunar rock and regolith is constructed from minerals and glasses [1]. The dominant lunar silicates are pyroxenes $(\text{Ca},\text{Fe},\text{Mg})_2\text{Si}_2\text{O}_6$, plagioclase feldspar $(\text{Ca},\text{Na})(\text{Al}_2\text{Si})_4\text{O}_8$, and olivine $(\text{Mg},\text{Fe})_2\text{SiO}_4$. The highlands are dominated by plagioclase, anorthite $(\text{CaAl}_2\text{Si}_2\text{O}_8)$ with some pyroxene $(\text{Mg},\text{Ca},\text{Fe})\text{SiO}_3$ and olivine $(\text{Mg},\text{Fe})_2\text{SiO}_4$. The mare is basaltic with varying proportions of plagioclase, pyroxene and olivine with up to 20% ilmenite FeTiO_3 and/or 10% spinel $(\text{Fe},\text{Mg})(\text{Cr},\text{Al},\text{Fe},\text{Ti})_2\text{O}_4$. Many minerals exhibit a range of compositions which are flanked by two or more end members. Lunar olivine is concentrated in mare soil being of low abundance in highland soils. Lunar olivine varies from Mg_2SiO_4 (forsterite) to Fe_2SiO_4 (fayalite) with intermediate solid solutions $(\text{Mg},\text{Fe})_2\text{SiO}_4$ and is enriched in Cr compared to terrestrial olivines. Lunar plagioclase is dominated by the calcium end member, anorthite $(\text{CaAl}_2\text{Si}_2\text{O}_8)$ but depleted in the sodium end member, albite $(\text{NaAlSi}_3\text{O}_8)$. The lunar highlands represent the original lunar crust of anorthositic rock dominated by the mineral anorthite $\text{CaAl}_2\text{Si}_2\text{O}_8$, i.e. rich in Ca and Al. Lunar mare represent more recent magma outflows of basalt comprising plagioclase (primarily anorthite), orthopyroxene $(\text{Mg},\text{Fe})\text{SiO}_3$, clinopyroxene $\text{Ca}(\text{Fe},\text{Mg})\text{Si}_2\text{O}_6$, olivine $(\text{Mg},\text{Fe})_2\text{SiO}_4$, and ilmenite FeTiO_3 , i.e. rich in Fe, Ti and Mg. Pyroxene has three end members MgSiO_3 (enstatite), CaSiO_3 (wollastonite), and FeSiO_3 (ferrosilite). Orthopyroxenes have the two end members, enstatite and ferrosilicate. All other pyroxenes are clinopyroxenes. Pyroxenes are ubiquitous in lunar regolith – primarily, clinopyroxene in the mare regions but both clinopyroxene and orthopyroxenes occur in the highlands. Magnesium pyroxenes and enstatite are depleted compared to Earth. KREEP rocks are enriched plagioclases that occur in localised regions. Sodium feldspars and potassium feldspars are rare as are granites, silica, clays, micas and amphiboles which require water for their formation. Metal oxides are abundant especially in the mare basalts. The Fe content of mare basalt feldspar is much higher than highland anorthositic feldspar. The commonest oxide is ilmenite $(\text{Fe},\text{Mg})\text{TiO}_3$ followed by spinels. Spinels are present but only as minor constituents of lunar soil. Spinel end-members include spinel $(\text{MgAl}_2\text{O}_4)$, ulvöspinel $(\text{Fe}_2\text{TiO}_4)$, chromite $(\text{FeCr}_2\text{O}_4)$ and hercynite $(\text{FeAl}_2\text{O}_4)$. Ti-rich basalts have higher than 6% TiO_2 by weight in the form of ilmenite and are found in Oceanus Procellarum and Mare Tranquillitatis on the nearside. Iron metal occurs widely in lunar regolith but at low concentrations <1% as Fe or NiFe nanophase grains from meteoritic sources. Troilite is ubiquitous but

in low concentrations and is associated with ilmenite and spinel. This yields a characteristic elemental abundance in Table 1.

Solar wind has impregnated the lunar regolith with volatiles. Lunar regolith comprises a repository of solar wind-derived volatiles in the upper 2-3 m due to gardening by impacts [2]. The abundance of solar wind volatiles in regolith is directly correlated with the duration of its exposure (maturity) [3]. Maturity is indicated by the degree of glass agglutination and degree of nanoparticle Fe^0 metallicity to FeO . Carbon mixture comprises primarily CO and smaller but similar amounts of CO_2 and CH_4 . Nitrogen is primarily in the form of N_2 in similar amounts to CH_4 . Sulphur is released on heating as both H_2S and SO_2 . All F and Cl are released as HF and HCl respectively. Noble gases such as Ar are in trace amounts ($3.1 \times 10^{-4} \text{ cm}^3 \text{ STP/g}$ for ^{36}Ar). ^3He enrichment in the smallest grains of high TiO_2 (ilmenite) deposits by a factor of 100 favours prior separation of the $<20 \mu\text{m}$ ilmenite fraction [4]. He^3 is regarded as potentially valuable as a nuclear fusion fuel for D^3He reaction as it generates fewer neutrons than other fusion fuels. It is rare on Earth (estimated at around $2 \times 10^4 \text{ kg}$) – the global lunar inventory is estimated at $6.5 \times 10^8 \text{ kg}$ [5]. Heating to 700°C yields releases almost all the volatiles. Fractional distillation requires a vertical fractionating column to use density as a means of component separation [6]. The mixture is heated at the bottom of the column from which vapours rise and condense towards the top of the column. The column may be packed or plated with sieve trays to permit vapour flow upwards but reducing liquid flow downwards. Although lunar gravity is one-sixth that of Earth, the vapour-liquid thermodynamics within the fractionating column is the same such that gas velocity is given by:

$$v = \frac{Q}{A} = C \sqrt{\frac{\rho_L - \rho_G}{\rho_G}} \quad (1)$$

where Q=volumetric gas flow rate, A=column area, C=flooding constant, ρ_L =liquid density, ρ_G =gas density. It is the column area that must be adjusted to the Moon:

$$\frac{A_M}{A_E} = \sqrt{\frac{g_E}{g_M}} \quad (2)$$

Hence, the lunar cross section diameter must be 1.6 times that of an Earth column diameter for similar performance.

Table 1. Lunar resources (adapted from Taylor & Martel 2003 [7])

Element	Source	Concentration (average-measured max)
H	Regolith volatile	50-150 $\mu\text{g/g}$
^3He	Regolith volatile	4-30 ng/g

⁴ He	Regolith volatile	14-100 µg/g
C	Regolith volatile	124-300 µg/g
N	Regolith volatile	81-150 µg/g
Fe	Mare basalt	150-170 mg/g
Ni	Regolith	250-330 µg/g
Co	Regolith	35-68 µg/g
W	Regolith	0.37-1.95 µg/g
Cr	Mare basalt	2-10 mg/g
Ti	Mare basalt	70-80 mg/g
Al	Highland anorthosite	180 mg/g
K	KREEP	8-18 mg/g
P	KREEP	6-22 mg/g

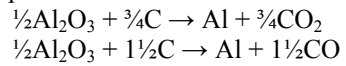
3. Industrial Ecology

Sustainability must be built into human exploration and colonisation goals upfront as a design requirement, not as an ad hoc afterthought, in much the same way as planetary protection is built into robotic exploration missions [8]. Sustainability is built on two pillars: (i) dematerialisation through the minimisation of material consumption; (ii) detoxification of waste. Industrial ecology addresses (ii) by converting waste in resources. The IPAT equation quantifies the impact I to be minimised – it is a complex function of the cost of launch of assets from Earth: $I=PAT$ where P=population of industrial products produced by deep ISRU, A=accumulative resource units consumed per product produced (specific mass), T=impact per resource unit consumed (amount of waste). To reduce A requires dematerialisation and to reduce T requires detoxification. Industrial ecology seeks to reduce impact T through recycling. Self-replication enforces minimisation of A through material and energy closure. Industrial ecology minimises the waste of one process by feeding it as input to other processes. It is of course highly desirable to achieve 100% closed loop recycling. Furthermore, there is a requirement for cradle-to-cradle sustainability which requires recycling at end-of-life – the recycling of 3D printed powder feedstock provides such a facility. FFC Cambridge is central to the minimisation/detoxification of waste by its yield of high purity metal.

4. Inexorability of Electrolysis

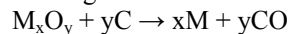
Electrolytic methods of mineral oxides tend to output higher product yields with higher purity than thermochemical reduction. Electrolysis is a highly versatile mode of chemical processing which is widely adopted on Earth. Aluminium production on Earth involves the mining of bauxite, production of alumina from bauxite (Bayer process) and alumina reduction to

Al metal electrolytically (Hall-Heroult process). Bauxite is typically up to 40% alumina, 10-30% Fe_2O_3 , 5-20% SiO_2 and around 2-5% TiO_2 . The Bayer process dissolves bauxite in NaOH solution to precipitate Al(OH)_3 which is calcined to produce Al_2O_3 . Molten NaOH could also be used to treat ilmenite to preferentially dissolve TiO_2 leaving insoluble Fe_2O_3 . Alumina is passed into a Hall-Heroult electrochemical cell as Al_2O_3 dissolved in molten Na_3AlF_6 (cryolite) solution at 960°C for electrolytic reduction using graphite electrodes which are consumed:

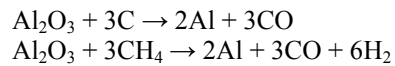


Molten Al is tapped at the bottom of the cell. Currently, Al production produces CO_2 greenhouse gases (0.5 kg C per kg Al produced) resulting from oxygen release at graphite anodes and toxic perfluorocarbon (such as CF_4 and C_2F_6) emissions due to reactions with molten cryolite.

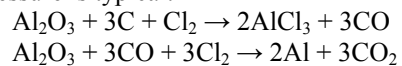
Aluminium production is highly energy intensive with 30% of its production cost being energy, two-thirds of which is used in the Hall-Heroult process [9]. The Hall-Heroult process consumes 14 kWh/kg accounting for 75% of the total energy consumption of aluminium production (electrolyte heating is electrical). Carbothermal reduction of bauxite with graphite powder has been proposed to reduce this energy consumption by 30% [10]. It also eliminates F compound pollutant production. Carbothermal reduction is a general method of reducing metal oxides:



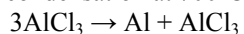
Carbothermal reduction is the basis of blast furnace processing of iron ore to yield iron and steel. Carbothermal reduction of alumina may be represented as:



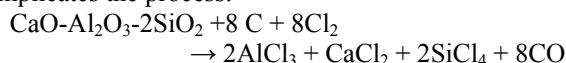
This requires high temperatures of 2060°C and 1500°C respectively due to the high stability of Al_2O_3 . This approach offers poor yields due to the formation of metal carbide constituents. Two-stage processing involving the formation of Al_4C_3 in Al_2O_3 slag at 2200°C (or 1500°C at 1000 Pa) requires subsequent electrolysis at 2000°C to yield Al metal. Stepped heating of bauxite at 1100°C and 1200°C yields metallic iron and ferroalloy of Al-Si (with carbides of Ti, Si and Al) respectively. An indirect rather than direct carbothermal process of alumina reduction involves the production of intermediate Al compounds such as AlCl_3 followed by the Alcoa electrolytic process. Intermediate product techniques include carbochlorination, carbonitridation and carbosulphidation [11]. Carbochlorination begins at 1600°C under 150 Pa pressure is typical:



Carbochlorination of lunar anorthite follows a similar principle though reduction of oxides will yield Ca-Al-Si alloy. Prior separation of CaO may be warranted if cement production is implemented. Extraction of Al from AlCl₃ may be either through low yield condensation or through electrolysis. AlCl₃ vapour may be passed through Al alloy above 1000°C followed by condensation at 700°C:



Formation of CaCl₂ and SiCl₄ from anorthite complicates the process:



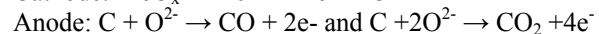
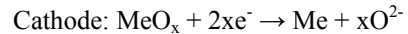
The Alcoa electrolytic process dissolves AlCl₃ in NaCl-LiCl electrolyte at 730°C to generate Al (at much lower temperature than the Hall-Heroult process) without the consumption of carbon electrodes (with an energy consumption of 9 kWh/kg Al). Chlorine gas may be recycled for the carbochlorination step. Fluorination has been proposed as the intermediate metal compounds [12] but this involves more corrosive and severe reagents. An alternative is the use of ionic liquids - organic salts that dissolve oxides into a solution at 150-160°C from which electrolysis can liberate oxygen at the anode and metals at the cathode [13]. For example, alumina and bauxite can be dissolved in 1-ethyl-3-methyl-imidazolium hydrogen sulphate at 210°C [14]. Ionic liquids however are impractical for lunar application.

Hence, all roads lead to the royal road of electrolysis. Since the development of the two-stage Bayer/Hall-Heroult processes, aluminium has displaced cast iron, steel, tin-plate, cast zinc, copper tubing, timber, glass and cardboard. However, for lunar application, it is an open question whether aluminium production is necessary as its functions can be substituted for with iron alloys (including kovar). Conversely, aluminium production would not eliminate the need for subsurface access to meteoritic material such as tungsten because its low concentration in surface regolith. Nevertheless, electrolytic processes are favoured for lunar application. Molten regolith electrolysis involves melting regolith at 1600°C and then applying a potential difference between the two electrodes. Oxygen is evolved at the anode and metals at the cathode (iron, silicon, etc). Molten oxide electrolysis is much favoured because it requires no reagents and yields high purity but it requires considerable energy. Pt group metals such as Ir for the anode exhibit potential long life durability.

5. FFC Cambridge Process

The FFC Cambridge process is an electrolytic process which reduces mineral oxides to 99% pure metal. The raw mineral oxide is pre-processed by powdering, compacting and sintering into a cathode rod.

It is inserted into an electrolytic cell with molten salt CaCl₂ as the electrolyte at 900°C in conjunction with an appropriate anode. Nominally, a graphite electrode is employed, yielding CO/CO₂ gas evolved at the anode. At the appropriate electrical potential (3 V being typical), the cathode is reduced to sintered solid pure metal releasing O²⁻ ions into the electrolyte solution which are transported to the anode to form CO/CO₂ gas which is released:



Any metal oxide can be reduced in this manner. Reduction of the metal oxide occurs in the solid state without melting yielding reduced energy consumption. The electrolyte is not consumed (except through cathode removal due to its porosity) but the anode is, and must be replenished – essentially, this is an electrolytic version of carbothermal reduction of mineral oxides. Capturing and recycling the CO/CO₂ gas and reducing it to carbon will be necessary to conserve the carbon. To obviate against the loss of carbon, an inert anode would be desirable to release O₂ gas directly (2O²⁻ → O₂ + 2e⁻) [15]. SnO₂ doped with 2% Sb₂O₃ and 1% CuO was successful as an inert anode but it eroded rapidly; a more promising anode was a solid solution of calcium titanate and calcium ruthenate (CaTi_xRu_{1-x}O₃). The O₂ released as a waste product may be stored for human consumption or as propellant oxidiser. Thermal heating to the modest 900°C could be accomplished through solar concentrators such as Fresnel lenses. We have demonstrated Fresnel lens smelting of Al alloy at 800°C under field conditions (Fig 1).

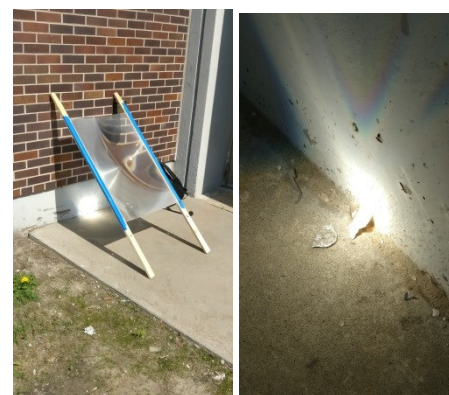


Fig 1. Smelting of Al alloy pieces using a Fresnel lens-based solar concentrator

Distribution of the thermal energy through the electrolytic bath however may prove challenging. Electrical energy may be supplied through thermionic conversion at 10-15% efficiency.

6. Naïve FFC Cambridge Process

We investigate two options for FFC Cambridge process on lunar minerals. First, we discuss the application of the technique to raw lunar minerals to yield mongrel alloys. Commonly used alloys typically comprise a single dominant metal with the addition of small amounts of other metals but mongrel alloys are dependent on the initial constituents of the mineral. Nominally, the FFC Cambridge process can be used to reduce lunar ilmenite (FeTiO_3) from mare regions to FeTi alloy. General FeTi alloy may be employed for general purpose structures; ferrotitanium alloy (45-75% Ti) may be used for oxidant mop-up purification, or as a pyrotechnic powder fuel with O_2 oxidant. Its oxygen-scavenging properties may not prevent its general use on the Moon but it should not be employed where free O_2 is in proximity.

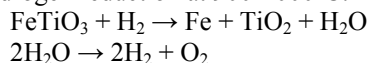
The FFC Cambridge process can be used to reduce lunar anorthite ($\text{CaAl}_2\text{Si}_2\text{O}_3$) from highland regions to AlCaSi alloy. AlCaSi alloy may be used for general purpose structures. Aluminium-silicon is a common filler metal used for brazing aluminum. Brazing involves melting a lower melting point filler to join two metal parts in a gas flux to prevent oxidation (unnecessary in a vacuum). Nickel alloy is used for joining steels while cobalt is used for joining superalloys but brazing does not have the high strength of a welded joint. AlSi alloys (20-50% Si) are used for casting and welds whereby Si provides fluidity with low shrinkage. As they solidify, the Si particles provide high wear resistance and low thermal expansion. To compensate for Fe contamination, Ni and Co may be added to improve strength. AlSi alloy exhibits lower viscosity than pure aluminium and is suitable for casting or powder metallurgy. Etching yields a hardened, highly wear-resistant silicon precipitate that is porous enough to retain oil that is suitable for linerless reciprocating components. Hence, silumin (3-25% Si) alloy is an AlSi alloy used for high durability applications such as in the lining of moving parts for machines such as pistons.

The FFC Cambridge process may reduce lunar olivine (Mg_2SiO_4) from crater regions directly to MgSi alloy. MgSi alloys may be used for general purpose structures; small amounts of Mg₂Si alloy are added to Al to produce high strength Al alloy.

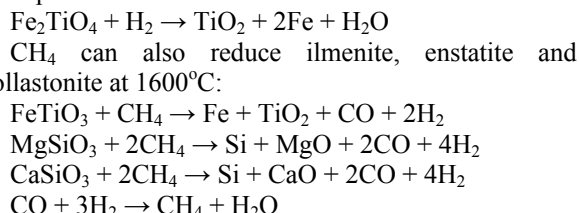
The properties of these mongrel alloys – FeTi, AlCaSi and MgSi - needs to be investigated further, particularly for general purpose structural applications. There is a general requirement for tensile structures to complement current interest in 3D printing compressive structures on the Moon [16,17]. The specialised applications of the mongrel alloys are insufficiently useful to justify the use of the FFC Cambridge process directly to unprocessed lunar minerals.

7. Smart FFC Cambridge Process

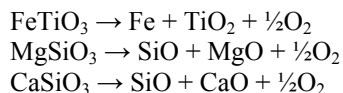
The versatility of the FFC Cambridge process however is best realised in the reduction of pure metal oxides. Hence, we must employ thermochemical pre-processing to lunar minerals to reduce them to pure metal oxides. Lunar ilmenite may be reduced through hydrogen reduction at 900-1000°C:



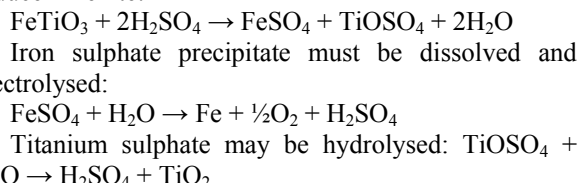
The product is a solid sponge of rutile and iron which could either be hammered out or ground into powder (such in a ball mill) to separate out the respective constituents. Alternatively, further heating to 1600°C allows bleeding of molten Fe from TiO_2 but the TiO_2 sponge will retain some Fe unless further processed. Some residual impurities including iron may be useful in producing titanium alloys. The water vapour is electrolytically separated into H_2 which is recycled and O_2 which is stored for subsequent use. Ulvöspinel can also be reduced in a similar manner:



The disadvantage is that it requires CH_4 but CO can be recycled. Reduction of metal oxides with hydrogen or methane is the simplest approach but the resultant purity is limited. Vapour phase pyrolysis involves decomposition and vaporisation of mineral oxides above 2000°C:



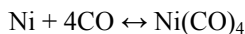
Vapour phase pyrolysis is more versatile requiring no chemical reagent but requires very high temperatures. Hot concentrated sulphuric acid can reduce ilmenite:



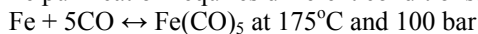
The acid may be recycled. The use of acids such as HF, HCl or H_2SO_4 requires import of such corrosive reagents from Earth and yield complex reaction sequences. Nevertheless, there are a host of pre-processing options.

Iron is a versatile metal that lends itself to multiple applications. Wrought (pure) iron is tough and malleable, suitable for tensile (or compressive loads if designed appropriately such as I beams) in structures. Steel requires the addition of small amounts <2% carbon as the dominant additive. Tool steel (<2% C and

9-18% W) is durable steel used for cutting tools for low wear. Silicon steel (up to 3% Si) is electrical steel used for electromagnet and motor cores. Kovar (53.5% Fe, 29% Ni, 17% Co, 0.3% Mn, 0.2% Si and <0.01% C) is a type of fernico alloy with high electrical and thermal conductivity as a replacement for copper and/or aluminum conducting wire. Permalloy (20% Fe and 80% Ni) provides magnetic shielding around motor devices to protect adjacent electronics from stray magnetic fields. The more exotic materials may be sourced from impact craters exhibiting magnetic anomalies indicating the existence of impactor metals [18]. Kamacite/taenite (NiFe alloys with 4-30% Ni) contaminated with ~0.5% Co is the major constituent in nickel-iron meteorites. Ni and Fe may be extracted through the Mond process. For Ni, this requires reacting CO with an S catalyst at 40-80°C and 1 bar to form nickel carbonyl gas which is then reversed at 230°C and 60 bar:



Fe purification requires different conditions:



The S catalyst may be recovered at 750-1100°C from troilite FeS in meteoritic inclusions, lunar regolith (~1%) or lunar volatiles. CO may be derived from lunar volatiles or the FFC Cambridge process if using a graphite anode. Removal of Ni and Fe concentrates the Co fraction of the residual ore. Alternatively, Co may be extracted by roasting with S in oxygen to convert cobalt into cobalt sulphate which is soluble in water. Co may then be extracted electrolytically. Meteoritic NiFe alloys are also enriched in W microparticle inclusions at a concentration of 0.1-5 µg/g. Following grinding, the high density of W at 19.3 lends itself to extraction by froth flotation.

Once ilmenite has been reduced to rutile TiO₂, FFC Cambridge process may be employed to yield near pure Ti (Fig 2a and b) – indeed, the FFC Cambridge process was originally developed to extract Ti from rutile to replace the Kroll process.

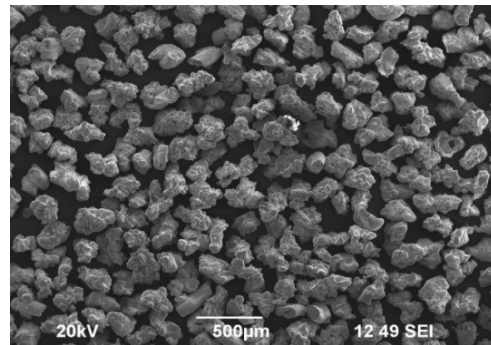
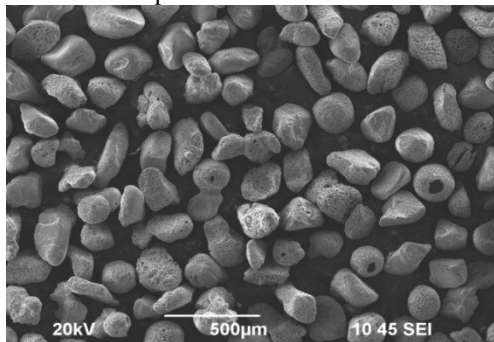
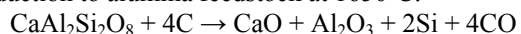
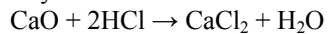


Fig 2. (a) rutile feedstock input to FFCC; (b) Ti metal product output from FFCC

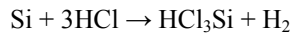
Anorthite may be subjected to carbothermal reduction to alumina feedstock at 1650°C:



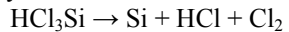
The mixture of metal oxides and silicon requires separation after powdering – the addition of Al metal powder at high temperature scavenges oxygen (by forming further Al₂O₃) and reduces CaO to Ca metal which may be tapped off as liquid above 842°C. Alternatively, CaO may be reacted highly exothermically with HCl to yield CaCl₂ electrolyte directly:



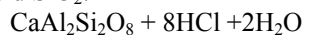
The reaction of powdered Si with HCl at 300°C yields volatile trichlorosilane liquid:



Removal of H₂ allows reversal to yield purified polysilicon:



Hence, chlorine is recycled. The alumina may be subjected to FFC Cambridge process to yield pure aluminium metal. An alternative treatment of anorthite is artificial weathering with HCl at room temperature to yield SiO₂:

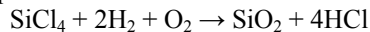


SiO₂ may be employed for fused silica glass production and for the production of quartz (piezoelectric sensing material). Aluminium chloride hexahydrate may be melted above 100°C to separate it from CaCl₂ and SiO₂ – it may subsequently be heated to yield alumina at 400°C:

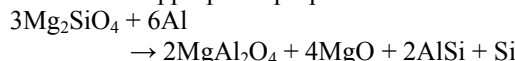


Silica and alumina may then be reduced separately through the FFC Cambridge process. Si may be employed as an additive to Fe for silicon steel. The artificial weathering reaction produces CaCl₂ as a source of FFC Cambridge electrolyte. Soda glass cannot be made on the Moon due to the paucity of Na but this is not an issue on Mars where NaCl is abundant. Aluminosilicate (57% SiO₂, 20% Al₂O₃, 12% MgO, 5% CaO) or fused silica glass are the only available options. It has been proposed that lunar aluminosilicate such as

anorthite be used as the basis for glass on the Moon - aluminosilicates have a melt temperature of ~1100-1350°C which is significantly lower than the 1700°C required of fused silica [19]. However, the moderate to high FeO content causes glass darkening which is undesirable for transparency so it would have to be removed. This may be accomplished through purification of alumina as the basis for glass-making to which the other components may be added in the required proportions. High purity SiO₂ can be enforced by heating in a H₂-O₂ flame in the presence of SiCl₄ vapour:



Olivine may be subjected to aluminothermic reduction in the appropriate proportions at 1000°C:



The MgO can be reduced by AlSi by continuing the reaction at 1000°C:



Molten Mg above 650°C enables it to be tapped from the refractory oxide. The FFC Cambridge process may reduce the MgAl₂O₄ spinel to MgAl alloy (such as magnallum as a lightweight corrosion-resistant alloy or solid fuel if ground) after separating it out from Mg, AlSi alloy and pure Si.

8. 3D Printing

3D printing is a versatile method of manufacturing that offers considerable versatility over traditional subtractive methods. 3D printing is an additive manufacturing process in which 3D structures are built up sequentially layer-by-layer. The most common 3D printing technique is fused deposition modelling (FDM) exemplified by the RepRap 3D printer [20] (Fig 3).

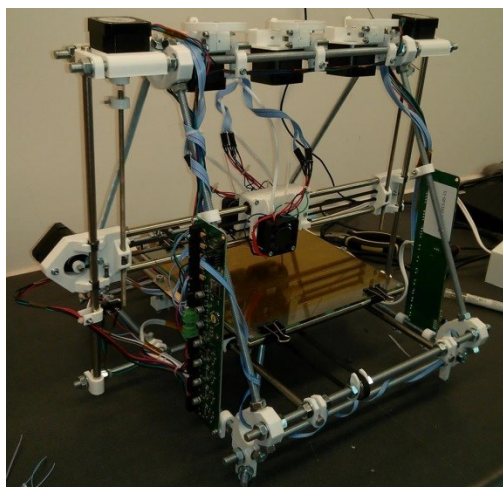
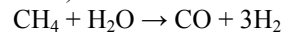


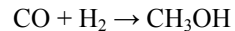
Fig 3. RepRap 3D printer

The Moon possesses regolith volatiles that may be used as raw material for the manufacture of plastics –

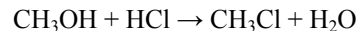
organic polymers may be rigid, elastic or plastic. Polymer moduli of elasticity falls in the range 10 MPa to 4 GPa compared with 50-400 GPa for metals. Tensile strength of polymers is 10 – 100 MPa compared with up to GPa for metals. Plastics have low fracture strength compared to metals. Plastics have poor response to high temperatures due to a reduction in tensile strength and increased ductility. Hence, metals are better suited to load-bearing, stiff structures while plastics are best employed as elastomers. i.e. silicone plastics. To minimise carbon consumption, silicone plastics have a silicone-oxygen backbone rather than a C backbone. Silicone plastics have advantages over hydrocarbon plastic in that they are UV radiation resistant and possess higher operational temperature resistance (up to 350°C). While organosilazanes are used for specialised protective coatings and adhesive cements, organosiloxanes are used more widely – motor lubricants, motor insulation, sealants, adhesives and coolant. This favours siloxanes for their wide functionality. Siloxane manufacture begins with the formation of syngas from methane and water (lunar volatiles) at 850°C and 4 MPa over a Ni catalyst:



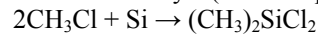
Syngas is converted to methanol (or higher alcohol) at 250°C and 5-10 MPa over an alumina catalyst:



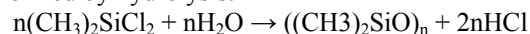
Chloromethane is formed by the action of HCl on methanol at 340°C over an alumina catalyst:



Dialkyl dichlorosilane is formed from the reaction of chloromethane with Si at 320-370°C and 1-5 bar in the presence of a catalyst (Rochow process):



It is an open question whether Ni could replace the more commonly used Cu catalyst in the Rochow process as copper is not available on the Moon. For example, the Fischer-Tropsch reaction requires a H₂:CO ratio of 2 for a Co catalyst but an Fe catalyst can tolerate a lower ratio. However, Fe-based catalysts also require alkali metal promoter such as K and ceramic support such as SiO₂. The most effective catalysts are CoFe/TiO₂, Co/TiO₂, CoNi/TiO₂, NiFe/TiO₂ and FeCo/SiO₂ for Fischer-Tropsch reactions. Intriguingly, lunar dust has been demonstrated as an effective catalyst for Fischer-Tropsch synthesis [21]. The Rochow process catalyst requires further investigation. Finally, the simplest silicone oil, polydimethylsiloxane (PDMS) is formed by hydrolysis:



HCl is recycled. Hence, silicone plastics may be manufactured from lunar volatiles given a source of Cl reagent. Silicone plastic is suitable for 3D printing by FDM. Furthermore, silica-based ceramics (polymer-derived ceramics) may be derived from pyrolysis of silicone polymers (organosilazanes or organosiloxanes)

- this permits shaping or 3D printing of the polymers prior to thermal conversion to ceramics which offer high temperature stability to 1500°C (increased by 2000°C with the addition of Al by the sol-gel process) [22]. Polysiloxanes (RSiO_{1.5}) can also be transformed into piezoresistive SiOC ceramics through pyrolysis in an inert atmosphere at or above 1400°C – the high temperature is necessary for piezoresistivity with an extremely high sensitivity of ~145 [23]. Hence, ceramic structures can be 3D printed in polymer form. RepRap represents a first step towards self-replicating machine in that it can print most of its plastic components (and potentially silica-based ceramics). However, it cannot print its metal components. A derivative of the RepRap has been developed that employs a welding head to print metal though its accuracy is poor [24]. Our interest here is in higher performance metal 3D printing.

The product of the FFC Cambridge process is a metal alloy powder that may serve as feedstock for 3D printing such as selective laser sintering/melting (SLS/SLM) (Fig 4). SLS/SLM offers the ability to deal with multiple materials – metals, plastics, ceramics and glasses.

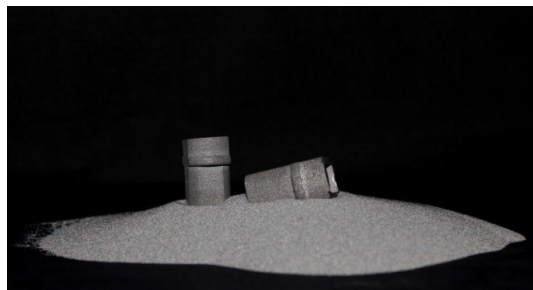


Fig 4. SLS-printed structures from FFC Cambridge-derived Ti powder

Solar concentrator-based sinterers offer an alternative technique more suited to lunar application but without the high power precision of the laser. Silica with a melting point of 1600°C is usually sintered in a high temperature furnace but the addition of Ca, Al, Mg and Cl lowers the melting temperature to 500-700°C to permit low power sintering at 200 W [25]. Metal gears have been constructed from moulds of sand mixed with sodium silicate sintered using low powered lasers. Sodium silicate solution permeates the sand mould for superior finish.

Alternatively, the powder may be sintered into rods for electron beam additive manufacturing (EBAM) [26] (Fig 5). Most metals – steel, nickel alloys, cobalt alloys, copper-nickel alloys, aluminium alloys, titanium alloys, tantalum, and tungsten but not zinc, cadmium or magnesium alloys - can be electron beam processed but non-metals are not suited as the electron beam needs to couple electrically to the material.

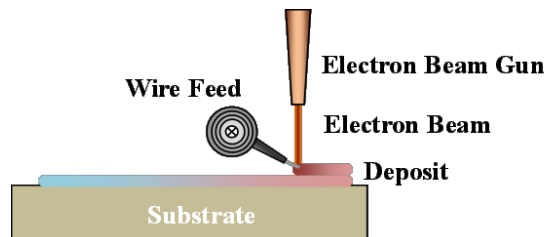


Fig 5. Electron beam additive manufacturing

EBAM is of particular interest because of its construction being based on the electron gun with implications in developing self-replicating machines [27]. In any case, metal printing typically requires high energy projection such as electron beam sintering/melting, laser sintering/melting or variants on these processes. The high energy deposition can cause residual stresses and layer warping. For example, EBAM imposes 2000°C peak temperatures followed by rapid cooling. Pre-heating of the work platform between the sample recrystallisation and melting temperature alleviates these high thermal gradients and consequent internal stresses.

Of particular interest is multi-material 3D printing of which there have been several demonstrations using freeform fabrication. A zinc-air cell comprising multiple materials was manufactured through a similar process to 3D printing [28]. A customized Cartesian gantry robot configuration of 3D printer was used to implement freeform deposition with different cartridges. Two plunger-based extruder deposition heads with integral heaters were dedicated to plastic/metal and liquid/pastes respectively. The material for each printer head was easily changed by substituting different syringe cartridges in each extruder head. The zinc-air battery comprised multiple layers with Zn anode particles in a KOH solution surrounded by a silver paste layer, carbon black/MnO₂ cathode catalyst in KOH solution electrolyte, a pre-cast separator layer of insulating ceramic foam overlying an air (oxygen) cathode surrounded by a silver paste. The assembly was mounted within an ABS plastic casing with copper wiring to the electrodes. In addition, a passive flexure joint of silicone plastic between rigid ABS plastic members was fabricated. The silicone was impregnated with carbon black while embedded wires of silver/methylcellulose paste were also fabricated within the joint – a simple actuator.

9. 3D Printing Motors

As well 3D printing metal structures, it would considerably widen the applications of 3D printing if mechatronic components could be 3D printed [29] – indeed, such as a facility opens up the possibility of 3D printing robots and other kinematic machines. Other such kinematic machines include 3D printers, milling

machines, lathes, drills, etc. This effectively constitutes a universal construction capability – a universal constructor is a machine that, given the appropriate resources, can construct any machine, including a copy of itself [30]. A major leap towards such a universal constructor would be demonstration that motors, electronics and sensors can be 3D printed.

To that end, we have been attempting to 3D print a number of motor designs. Initially, we 3D printed a variable reluctance motor because of its lack of brushes and simple construction – only the metal elements were not 3D printed (Fig 6).

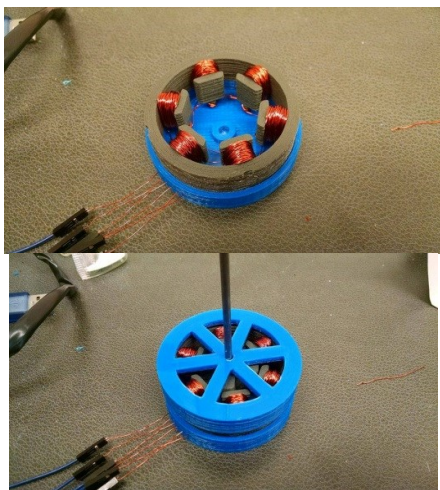


Fig 6. 3D printed switched reluctance motor

We then focussed on the general purpose DC electric motor to tackle the magnetic and electrical elements rather than just the structure. Beginning with the rotor, we have 3D printed a motor core comprising 50% iron filings (by mass) interspersed in a polylactic acid (PLA) matrix printed using the RepRap 3D printer from an off-the-shelf filament (Proto-Pasta magnetic filament) (Fig 7a). We then built a similar motor core with 50% iron filings (by volume) in PLA to increase the iron loading – this was manufactured using NRC's powder metallurgy facilities (Fig 7b). Although not 3D printed, it could be, and demonstrates that high metal loadings are feasible.

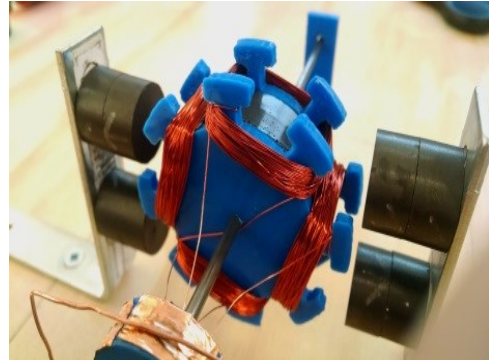
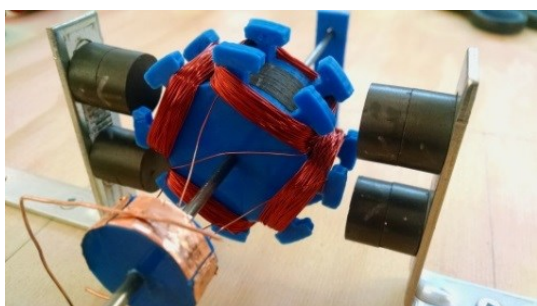


Fig. 7 (a) 3D printed PLA rotor with 50% iron powder by mass; (b) powder metallurgy-manufactured PLA motor with 50% iron powder by volume

We have since replaced the iron powder with magnetically-soft silicon steel powder to eliminate the minor detent problem on startup in the motors using iron powder. To address printing of the current-carrying wire coils, we have been photolithographically printing coils and testing them in a pancake “air” motor configuration (Fig 8a and b).

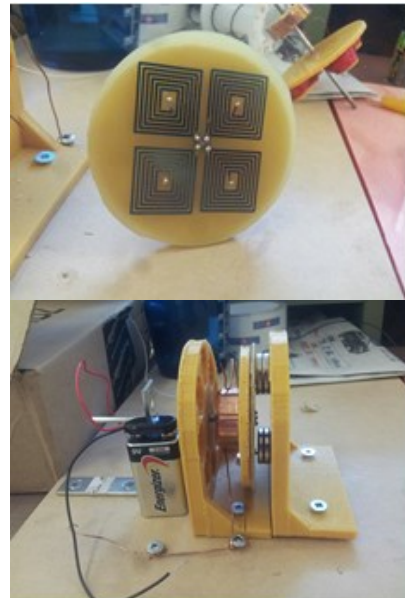


Fig 8. (a) Photolithographically-printed current-carrying coils (b) Pancake air motor test configuration

We attempted to construct a magnetically soft stator pair similarly to our rotor - a 3D printed stator of iron filings in PLA matrix but the stator magnetic field was too weak (to measure) even with 800 turns of wire (Fig 9a). A second stator pair of SLS-printed magnetically soft steel was constructed (Fig 9b) but its magnetic field of 3G was insufficient to generate torque.

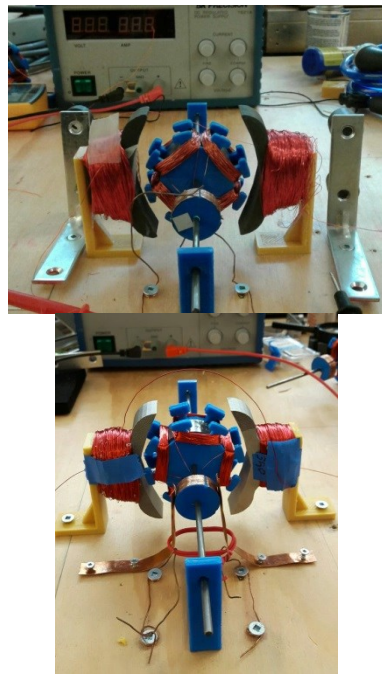


Fig 9. (a) Ineffective PLA-based stator (b) Ineffective magnetically soft steel stator

In order to reassess the stator design, we tested an off-the-shelf magnetically-soft ferrite stator system which yielded 20 G – sufficient to generate excellent torque (Fig 10).

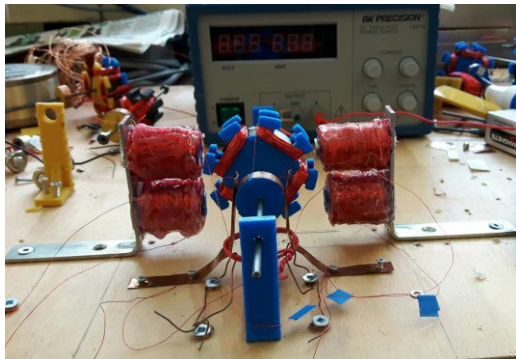
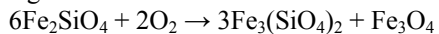


Fig 10. Non-3D printed ferrite stator demonstration

Magnetite (ferrite) may be manufactured from ferric olivine (fayalite) from chondritic sources on the Moon through oxidation at 400-700°C:



However, native magnetite may exist in some meteorites. The next steps will be to have a 3D printed ferrite stator integrated into an entirely 3D printed DC motor.

10. Conclusions

The combination of FFC Cambridge process and 3D printing offer a powerful approach to deep ISRU. Indeed, the FFC Cambridge process is best exploited

following pre-processing of raw materials to extract 99% pure metal elements. It operates in the solid state so the product is a metal powder that can be 3D printed directly or sintered into rod form. A variety of 3D printing techniques are suitable including laser, electron beam and solar concentrator forms. These two technologies will be critical imparting to the Moon a valuable infrastructure from which to establish lunar colonies.

Acknowledgements

The author would like to thank Abdurr Elaskri for his assistance with constructing the motors,

References

- [1] Papike J, Taylor L & Simon S (1991) "Lunar minerals" in *Lunar Sourcebook* (ed. Heiken G, Vaniman D, French B), Cambridge University Press, 121-155
- [2] Duke M, Gaddis L, Taylor J, Schmitt H (2006) "Development of the Moon" *Reviews in Mineralogy & Geochemistry* **60**, 597-656
- [3] Fegley B, Swindle T (1993) "Lunar volatiles: implications for lunar resource utilisation" in *Resources of Near-Earth Space* (ed. Lewis J, Matthews M, Guerrieri M), University of Arizona Press, 367-426
- [4] Johnson J, Swindle T, Lucey P (1999) "Estimated solar-wind implanted He-3 distribution on the Moon" *Geophysical Research Letters* **26** (3), 385-388
- [5] Fa W, Jin Y-Q (2007) "Quantitative estimation of helium 3 spatial distribution in the lunar regolith" *Icarus* **190**, 15-23
- [6] Petit D (1985) "Fractional distillation in a lunar environment" in *Lunar Bases & Space Activities of the 21st Century* (ed. Wendell M), Lunar & Planetary Institute, 507-518
- [7] Taylor J, Martel L (2003) "Lunar prospecting" *Advances in Space Research* **31** (11), 2403-2412
- [8] Debus A (2001) "Planetary protection aspects for in-situ and sample return exobiological experimentations" *Proc 1st European Workshop on Exo- and Astr-Biology (ESA SP-406)*, Frascati, Italy, 113-119
- [9] Botte G (2014) "Electrochemical manufacturing in the chemical industry" *Electrochemical Society Interface* (Fall), 49-55
- [10] Yeh C & Zhang G (2013) "Stepwise carbothermal reduction of bauxite ores" *Int J Mineral Processing* **124** (Nov), 1-7
- [11] Rhamdhani M, Dewan M, Brooks G, Monaghan B, Prentice L (2013) "Alternative Al production methods: part 1 – a review of indirect carbothermal routes" *Trans Institution of Mining & Metallurgy C*:

- Mineral Processing & Extractive Metallurgy* **122** (3), 87-104
- [12] Landis G (2007) "Materials refining on the Moon" *Acta Astronautica* **60**, 906-915
- [13] Marone M, Paley M, Donovan D, Karr L (2009) "Lunar oxygen production and metal extraction using ionic liquids" *LEAG Annual Meeting*, abstract no. 2034
- [14] Poulimenou N, Giannopoulou I, Panias D (2014) "Preliminary investigation of ionic liquids utilisation in primary aluminum production" *Proc Int Conf Mining, Material & Metallurgical Engineering*, Prague, paper no. 60
- [15] Schwandt C, Hamilton J, Fray D, Crawford I (2012) "Production of oxygen and metal from lunar regolith" *Planetary & Space Science* **74**, 49-56
- [16] Khoshnevis B, Bodiford M, Burks K, Thridge E, Tucker D, Kim W, Toutanji H, Fiske M (2005) "Lunar contour crafting – a novel technique for ISRU-based habitat development" *43rd AIAA Aerospace Meeting & Exposition*, Reno NV, paper no 538
- [17] Cesaretti , Dini E, De Kestellier X, Colla V, Pambagian L (2014) "Building components for an outpost on the lunar soil by means of a novel 3D printing technology" *Acta Astronautica* **93**, 430-450
- [18] Bland P, Artemieva N, Collins G, Bottke W, Bussey D, Joy K (2008) "Asteroids on the Moon: projectile survival during low velocity impacts" *39th Lunar & Planetary Science Conf*, abstract no 2045
- [19] Landis G (2007) "Materials refining on the Moon" *Acta Astronautica* **60**, 906-915
- [20] Jones R, Haufe P, Sells E, Iravani P, Olliver V, Palmer C, Bowyer A (2011) "RepRap – the replicating rapid prototyper" *Robotica* **29** (Jan), 177-191
- [21] Cabrera A, Maple M, Asunmaa S, Arrhenius G (1976) "Formation of water and methane catalysed by lunar dust" *NASA Report N91-71212*
- [22] Riedel R, Mera G, Hauser R, Klonczynski A (2006) "Silicon-based polymer-derived ceramics: synthesis properties and applications – a review" *J Ceramic Society Japan* **114**, 425-444
- [23] Riedel R, Toma L, Janssen E, Nuffer J, Melz T, Hanselka H (2010) "Piezoresistive effect in SiOC ceramics for integrated pressure sensors" *J American Ceramics Society* **93** (4), 920-924
- [24] Anzalone G, Zhang C, Wijnen B, Sanders P, Pearce J (2013) "Low-cost open-source 3D metal printer" *IEEE Access* **1**, 803-810
- [25] Wang X, Fuh J, Wong Y, Tang Y (2003) "Laser sintering of silica sand – mechanism and application to sand casting mould" *Int J Advanced Manufacturing Technology* **21**, 1015-1020
- [26] Taminger K & Hafley R (2006) "Electron beam freeform fabrication (EBF3) for cost-effective near-net shape manufacturing" *NASA TM 2006-214284*
- [27] Ellery A (2016) "Are self-replicating machines feasible?" *AIAA J Spacecraft & Rockets* **53** (2), 317-327
- [28] Malone E, Rasa K, Cohen D, Isaacson T, Lashley H, Lipson T (2004) "Freeform fabrication of zinc-air batteries and electromechanical assemblies" *Rapid Prototyping J* **10** (1), 58-69
- [29] Ellery A (2016) "Progress towards 3D printed mechatronic systems" *Proc IEEE Int Conf Industrial Technology with Symp on 3D Printing*, Taipei, Taiwan, pp. 1129-1133
- [30] von Neumann J and Burks A (1966) *Theory of Self-Reproducing Automata*, University of Illinois Press, Champaign, Ill